# A Study of the Evolution of Mesoscale Convective Systems Using WSR-88D Data

ERIC R. HILGENDORF* AND RICHARD H. JOHNSON

*Department of Atmospheric Science, Colorado State University, Fort Collins, Colorado*

(Manuscript received 12 May 1997, in final form 27 October 1997)

ABSTRACT

While mesoscale convective systems (MCSs) are major contributors to severe weather and precipitation in the central United States, details of their evolution are still not fully understood. In particular, recent observational and modeling studies have indicated that many MCSs tend to exhibit an asymmetric precipitation pattern during the mature-to-later stages of their life cycles. However, to what extent and how this evolution occurs in all cases is still a matter of conjecture.

The recently established WSR-88D network has afforded the opportunity to investigate the evolution of MCSs in greater detail than has been possible in the past. As a preliminary effort in this direction, 13 MCSs having leading line-trailing stratiform structures that occurred over the lower Midwest during May and June 1995 have been studied. It is found that indeed there does appear to be an evolution of such MCSs toward asymmetry later in their life cycles; however, the nature of the evolution is complex. The trailing stratiform region develops an asymmetric pattern (stratiform precipitation located toward the northern edge of the MCS) well before the system reaches maturity. The convective line also evolves to an asymmetric pattern (the most intense convective cells concentrated along the southern end of the line), but the appearance of asymmetry occurs several hours later than it does in the stratiform component. The limited sample size, however, precludes definitive conclusions about the significance of this timing difference.

Contributions to asymmetry by hydrometeor advection in the along-line component of the flow aloft have also been inferred from sounding data. Results indicate that the system-relative, along-line flow in the pre-MCS environment is comparable to and often greater than the cross-line flow. This evidence suggests that *both* along-line and cross-line, system-relative flows, along with other processes (e.g., Coriolis effects), may contribute to an evolution toward asymmetry.

## 1. Introduction

During the summer months expansive cloud shields accompanied by heavy rainfall and strong winds move across the central United States. These mesoscale convective systems (MCSs) have a significant impact on agriculture (Fritsch et al. 1986) and often pose threats of severe weather such as hail, flash flooding, high winds, and tornadoes (Maddox 1983; Johns and Hirt 1987; Houze et al. 1990; Doswell et al. 1996). MCSs evolve over 3–6 h and longer, contain at some stage both convective and stratiform precipitation regions (Zipser 1982; Smull and Houze 1985; Knupp and Cotton 1987; Biggerstaff and Houze 1991), and typically attain horizontal dimensions of at least 100 km (Houze 1993).

For years, studies of MCSs have used radar and other mesoscale data sources to determine the precipitation structure of individual convective events as well as their thermodynamic and kinematic properties (Newton 1950; Fujita 1955; Ligda 1951; Newton and Newton 1959; Pedgley 1962; Sanders and Paine 1975; Sanders and Emanuel 1977; Houze 1977; Zipser 1977; Smull and Houze 1985). However, in most instances, the studies sampled only small fractions of the lifetimes of the MCSs, owing to the small dimensions of the observing networks. Nevertheless, in some cases the precipitation structure has been documented (Pedgley 1962). The first effort to synthesize findings for many storms actually occurred in connection with *tropical* MCSs (Leary and Houze 1979). Using radar data, Leary and Houze identified four stages in the life cycle of MCSs: formative, intensifying, mature, and dissipating. The precipitation structures depicted were three-dimensional and generally referred to the type of squall line having a leading-convective line and trailing-stratiform precipitation region (Houze 1977; Zipser 1977).

The first efforts to investigate the evolution of *midlatitude* MCSs using radar data were by Bluestein and Jain (1985) and Bluestein et al. (1987). They classified the precipitation structure during the formative stages of midlatitude squall lines, identifying four common modes of development: broken line, back building, broken areal, and embedded areal. In a later, comprehensive

* Current affiliation: Cooperative Institute for Research in the Atmosphere, Fort Collins, Colorado.

*Corresponding author address:* Dr. Richard H. Johnson, Department of Atmospheric Science, Colorado State University, Fort Collins, CO 80523-1371.
E-mail: rhj@vortex.atmos.colostate.edu

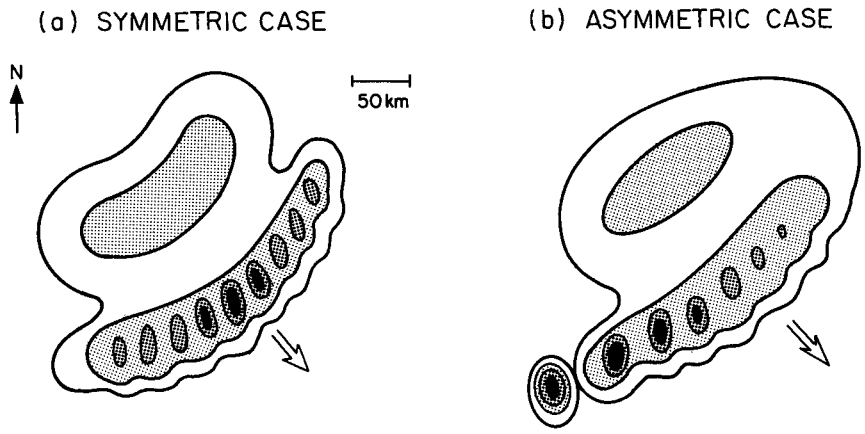


FIG. 1. Schema depicting (a) symmetric and (b) asymmetric types of leading line-trailing stratiform MCS precipitation organization (from Houze et al. 1990). Large vector indicates direction of system motion. Levels of shading denote increasing radar reflectivity, with most intense values corresponding to convective-cell cores. Horizontal scale and north arrow are shown.

study of midlatitude MCSs, Houze et al. (1990) established two classifications of MCS precipitation structures, symmetric and asymmetric (Fig. 1), based upon examination of 6 yr of warm-season radar data from Oklahoma City. Approximately ⅓ of the 72 MCSs were classified in each of these two categories, with the remaining third of the systems labeled unclassifiable.

The findings of Houze et al. (1990) were confirmed and extended by Loehrer and Johnson (1995) in their investigation of the precipitation structure and surface pressure features of MCSs that occurred during the 1985 Oklahoma–Kansas Preliminary Regional Experiment for Stormscale Operational and Research Meteorology [OK PRE-STORM; Cunning (1986)]. Loehrer and Johnson found that of the 12 PRE-STORM MCSs identified, 75% evolved from initially diverse structures to an asymmetric pattern during their mature stages. Four modes of initial organization were detected: linear, backbuilding, disorganized, and intersecting convective bands (Fig. 2). These patterns of evolution have been documented in detail in a number of observational studies of individual PRE-STORM cases (e.g., Rutledge et

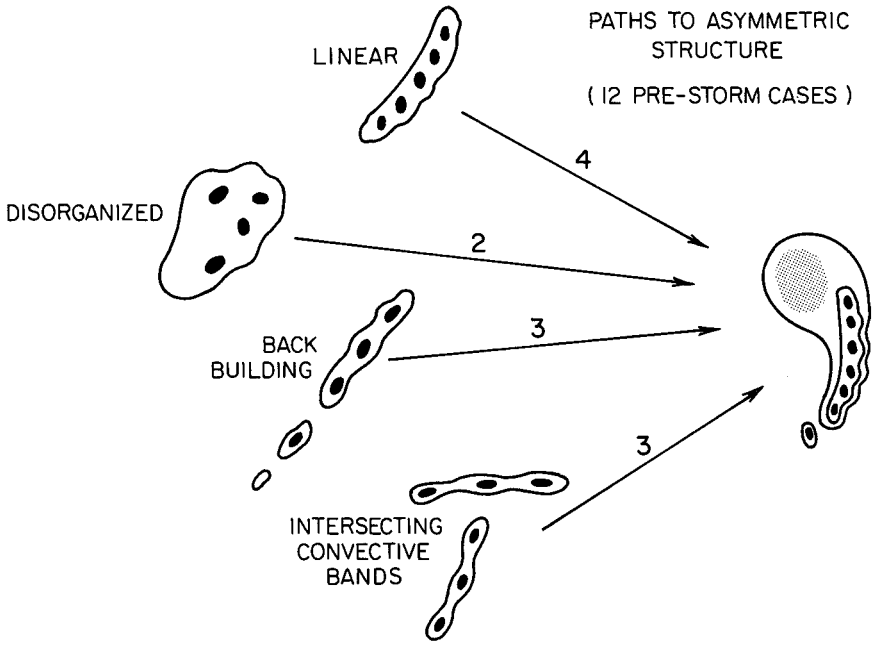


FIG. 2. Evolutionary paths to asymmetric structure for 12 MCSs during the 1985 PRE-STORM observed by Loehrer and Johnson (1995). Numbers above arrows indicate the number of systems observed to take that path.

al. 1988; Smull and Augustine 1993; Scott and Rutledge 1995).

Modeling efforts have been successful in simulating the observed evolution of MCSs (e.g., Skamarock et al. 1994). Starting with an initial, north–south, 200-km-long convective line, Skamarock et al. found that in the presence of Coriolis forcing, the evolving MCS developed an asymmetric structure in 6–10 h. This structure was attributed to two primary processes: 1) the Coriolis force acting upon the ascending front-to-rear flow in the convective line, turning it to the north and leading to an accumulation of hydrometeors and positively buoyant air there, and 2) the Coriolis force acting on the surface cold pool, driving cold air to the south and generating new cells preferentially on the southern end of the line. However, in the simulations of Skamarock et al. (1994), the role of the system-relative along-line component of the flow in producing asymmetry (Houze et al. 1990) was not investigated, an issue that will be addressed in this study. Davis and Weisman (1994) further examined the development of asymmetry from the standpoint of potential vorticity arguments.

Another proposed mechanism for creating asymmetric MCSs incorporates the low-level jet (LLJ). The LLJ has been identified as a recurrent feature in MCS genesis regions (Maddox and Doswell 1982; Maddox 1983) and is thought to provide essential moisture and warm air, which aids in destabilizing the genesis region and feeds the MCS (e.g., Brandes 1990; Trier and Parsons 1993). Smull and Augustine (1993) proposed that an MCS ingests northward momentum from the low-level jet into the updraft. At high levels of the troposphere this transported momentum carries detrained ice crystals northward from the convective towers, contributing to the formation of a stratiform region biased toward the north.

The horizontal precipitation structure of an MCS, which defines a system's symmetry, is an important factor in determining the distribution of rainfall and the possibility of flooding. All other things being equal, locations receiving both stratiform and convective rainfall have a greater risk of flooding than a location receiving only stratiform or convective rainfall (Doswell et al. 1996). Predictions of MCS symmetry (i.e., predictions for locations that would receive both stratiform and convective precipitation) could therefore aid in the warning of locations under the greatest threat of flash flooding. An important step in improving our forecasts of MCSs is to improve upon our understanding of the systems through observations.

Although there is accumulating evidence that many midlatitude MCSs tend to evolve toward an asymmetric pattern of the type defined by Houze et al. (1990), observational evidence of this process is incomplete. First, the Loehrer and Johnson (1995) study was only for a limited number of cases (12) and for a single season (May–June 1985). Second, while some degree of objectivity was involved in the MCS-compositing procedure of Loehrer and Johnson by defining storm quadrants based on storm direction of motion, the actual synthesis of the data from the various cases was inherently subjective. This paper represents a preliminary effort to improve upon some of these deficiencies by 1) examining MCS evolution over the central United States for yet another season and 2) increasing the level of objectivity in the procedures to synthesize and composite data to determine the characteristics of MCS evolution. Another important facet of this study is the use of observational tools, such as the upgraded National Weather Service (NWS) radar, WSR-88D, that are available to operational forecasters. It is recognized that the use of only one summer's worth of data represents a serious limitation to the present study; however, the work is intended to point toward the great potential value of WSR-88D for MCS characterization and evolution studies, and to initiate additional research along these lines.

In addition to documenting MCS evolution using WSR-88D data, NWS soundings are employed to examine system-relative flows in the pre-MCS environment. The object here is to see to what extent along-line system-relative flow, in addition to the cross-line component, contributes to storm asymmetry (Houze et al. 1990). Our findings are related to past modeling and observational studies that show that the precipitation structure, to a large degree, results from advective processes involving ice hydrometeors (e.g., Hobbs et al. 1980; Matejka and Hobbs 1981; Smull and Houze 1985; Biggerstaff and Houze 1991; Smull and Augustine 1993; Skamarock et al. 1994).

This paper begins with a discussion of the observing tools: WSR-88D imagery and NWS soundings. Section 3 describes how the tools are used to 1) choose which systems to study, and 2) isolate information that is important in documenting the characteristics of the horizontal precipitation structure. Section 4 defines thresholds for the two major precipitation structures (asymmetric and symmetric) to be applied to the WSR-88D data. Sections 5 and 6 discuss observations of the synoptic conditions using large-scale analyses, and mesoscale features as seen using WSR-88D imagery. Additionally, section 6 applies WSR-88D composites of the stratiform and convective regions to describe the precipitation evolution within those regions. The paper concludes with a study of the effects of advection on the precipitation structure evolution.

## 2. Data sources

### *a. Observational platforms*

There are two remote-sensing systems commonly used in operations to assess the precipitation characteristics of MCSs in real time: satellites and WSR-88D. WSR-88D, however, is better suited to define MCS precipitation structure and differentiate between convective and stratiform regions. Therefore, we used spatially composited WSR-88D reflectivity fields (base reflectivity scans from many sites merged together) that show the total horizontal structure of a system throughout its

evolution, something a single radar site rarely accomplishes due to the large horizontal extent and moderate-to-rapid movement of most MCSs.

The WSR-88D composites used in this study were provided by the Oklahoma Climatological Survey. The region covered by the composites is centered on north-central Texas and incorporates reflectivity from 39 WSR-88D sites (Fig. 3) with baseline scans inclined at an elevation angle of 0.5°. The composites comprise the standard six digital video integrator and processor levels (18–29, 30–40, 41–45, 46–49, 50–56, and ≥57 dB*Z*). The compositing algorithm uses the highest reflectivity available for a given location.

In addition to the precipitation structure, we observed the vertical distribution of horizontal winds through the depth of the troposphere. The source of the upper-air data is the NWS sounding network. The sounding observations included in the analyses were those that occurred within the paths of the MCSs. These soundings are assumed to be representative of the prestorm conditions for each MCS.

### *b. WSR-88D animation technique*

The procedure we used to document MCS evolution involves following the evolution of reflectivity patterns using continuity in time, a procedure which was expedited using *animations* of WSR-88D composites. WSR-88D animations provide an effective method of observing the entire evolution of MCS precipitation patterns and discriminating between convective and stratiform regions. They comprise continuous loops of radar reflectivity images at 30-min intervals. Although 5-min resolution imagery was available, a comparison of animations with 5-min resolution to those using 30-min resolution did not reveal any significant differences. Of course, 30-min images do not permit the sampling of the lifetimes of individual convective elements. However, the evolution of such features is not the focus of this study. Rather, the focus is the gross horizontal morphology of the overall MCSs, specifically the stratiform and convective components, both of which have lifetimes of many hours.

Because the distribution of hydrometeors within MCSs is not vertically homogeneous, (e.g., Leary and Houze 1979), sampling a system with a 0.5° elevation angle may yield ambiguity regarding the horizontal distribution of precipitation. This is especially true at long radar ranges where the majority of the power within the radar volume may extend above the main precipitation core and poorly sample the precipitation there. This problem in interpretation was mitigated in our analysis by using animations of WSR-88D composites, which spanned the entire lifetime of the MCSs. Through the use of animation, the MCSs were viewed from a variety of ranges and viewing angles, revealing the appropriate precipitation type for a given location within the MCS. We have selected the animation procedure (and thresholding techniques described below) for identifying stratiform and convective regions as opposed to using objective techniques (e.g., Collier et al. 1980; Steiner et al. 1995) because of animation's utility, flexibility, effectiveness as an interpretive tool, and especially its availability to operational forecasters.

## 3. Case selection and definitions

### *a. Case selection*

The MCSs included in this study are limited to systems that exhibited a leading line-trailing stratiform (ll–ts) structure[1] (Houze et al. 1990) at some stage during their development and had a horizontal dimension of 100 km in at least one direction. The MCSs generally moved toward the southeast and had a stratiform region to the west of a north–south-oriented convective line (see section 3b for definitions of stratiform and convective elements). Additionally, the MCSs identified occurred *completely* within the WSR-88D composite boundary (Fig. 3) between initiation and decay. Of the 30 MCSs that occurred within the composite area during May and June 1995, 18 (60%) exhibited ll–ts characteristics, which compares well with observations made by Houze et al. (1990) who found roughly two-thirds of the MCSs in their study were classifiable as ll–ts systems. Of the 18 ll–ts systems observed during May and June 1995 near the analysis region, 13 were fully sampled within the WSR-88D composite region and were subsequently used for this analysis (Table 1).

### *b. Definitions of convective and stratiform regions.*

We define the *stratiform region*[2] (Houze 1977; Zipser 1977) to be that part of the precipitation field separate from the convective line and having a nearly contiguous region of reflectivity ≥30 dB*Z* [roughly corresponding to 2 mm $h^{-1}$ (Doviak and Zrnić 1993)]. Table 2 lists the available reflectivity ranges and the precipitation type we assigned to each reflectivity value. Reflectivities of 18–29 dB*Z* are not used to identify the location of the stratiform region since anomalous propagation and clear air echoes (Doviak and Zrnić 1993) often associated with the nocturnal inversion frequently manifested themselves as reflectivities between 18 and 29 dB*Z*. Since 30 dB*Z* is the next lowest reflectivity level available, it is used as the stratiform threshold. This threshold is higher than the 15-dB*Z* threshold used in past work (e.g., Biggerstaff and Houze 1991; Loehrer and Johnson 1995). The reason our threshold differs

[1] The MCSs in our study were not analyzed to determine if they met all 10 of the ll–ts criteria defined in Houze et al. (1990). For the purposes of this study, the MCSs were considered ll–ts if they met most of the criteria, but were not required to meet all criteria.

[2] This region, although made up of predominantly stratiform rainfall, may contain some convective-scale features (e.g., Leary and Rappaport 1987).

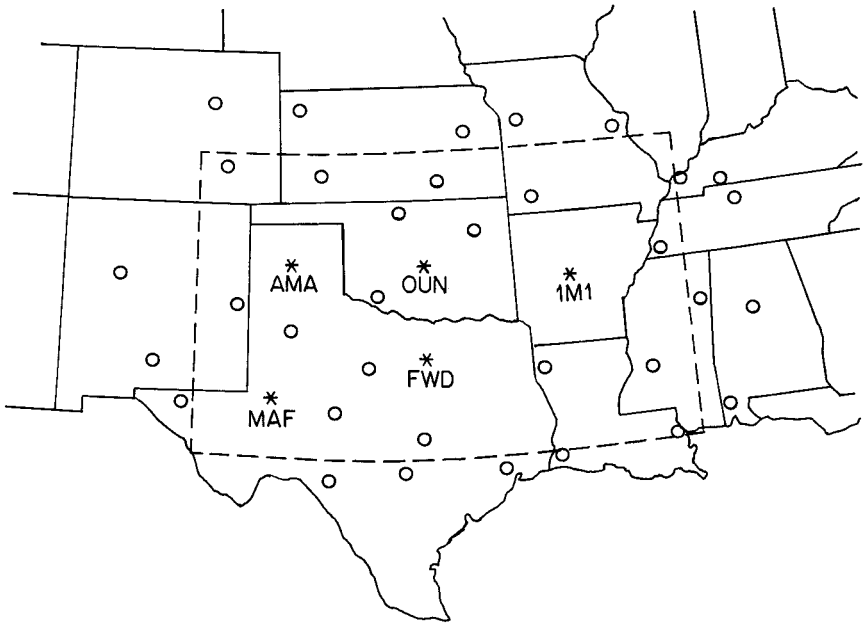


FIG. 3. Locations of WSR-88D sites (circles and stars) contributing to composites used in this study. WSR-88D composite boundary indicated by dashed lines, and sounding locations (stars) used for upper-air analysis along with three-letter NWS station identifiers.

from that used in previous work is that our focus is different. The intent of this research is to document the degree of symmetry (or asymmetry) of the evolving precipitation field, not to document the sizes of the precipitation fields as in Biggerstaff and Houze (1991) and Loehrer and Johnson (1995).

The upper limit of the lowest analyzed reflectivity range (30–40 dBZ) is close to reflectivity that may be considered representative of a convective region. In order to reduce the chance of analyzing a convective region as a stratiform region, we employ the conceptual model of an ll–ts MCS (Fig. 1) given in Houze et al. (1990) as a first guess of where to separate the stratiform and convective regions. This model of an ll–ts MCS has a distinct region of minimum reflectivity that separates the convective region from the stratiform. Thus, high reflectivity (e.g., isolated convective cells or bright bands due to melting) in what is known to be primarily stratiform precipitation is not misinterpreted as part of the convective line.

Armed with the conceptual model of an ll–ts MCS, the WSR-88D images are animated to provide additional confidence of our assessment of system structure. Single WSR-88D images do not provide enough information to confidently differentiate transient reflectivity patterns that are not part of the MCS from the more persistent patterns that compose an MCS. When viewing WSR-88D animations, the eye can isolate spatially and temporally contiguous patterns that compose an MCS. The animations are therefore indispensable for determining which low-reflectivity elements are part of the stratiform region. This animation technique is likewise applied to the documentation of the convective line.

TABLE 1. Date (all from 1995), time of initiation, start of maturity ($M$), duration between initiation and maturity ($\Delta t$) in hours rounded up to the nearest half hour, and time of the sounding used to represent ambient conditions for each MCS. The As and Bs represent the first and second MCS of that day, respectively. Times are in UTC for day of system (subtract 6 h to get local standard time).

| Date | Initiation | $M$ | $\Delta t$ (h) | Sounding (6 May) |
|---|---|---|---|---|
| 5 May | 1200 | 2345 | 11 | 0000 |
| 6 May | 0830 | 1530 | 7 | 1200 |
| 24 May | 2100 | 0400 | 7 | 0000 |
| 26 May | 0530 | 1600 | 10.5 | 1200 |
| 3 Jun A | 0900 | 1230 | 3.5 | 1200 |
| 3 Jun B | 0500 | 1130 | 6.5 | 1200 |
| 4 Jun | 0130 | 1030 | 9 | 0000 |
| 10 Jun A | 0630 | 1330 | 7 | 1200 |
| 10 Jun B | 1300 | 2100 | 8 | 1200 |
| 11 Jun | 2000 | 0730 | 11.5 | 1200 |
| 23 Jun | 1300 | 1800 | 5 | 1200 |
| 27 Jun | 2230 | 0430 | 6 | 0000 |
| 29 Jun | 0000 | 1330 | 13.5 | 1200 |

TABLE 2. Precipitation classification based on WSR-88D reflectivity. Reflectivities ≤29 dBZ were not analyzed in this study.

| Reflectivity (dBZ) | Classification |
|---|---|
| ≥57 | Most intense convection |
| 50–56 | Convective |
| 46–49 | Convective |
| 41–45 | Stratiform (rarely) |
| 30–40 | Stratiform |
| 18–29 | Not analyzed |

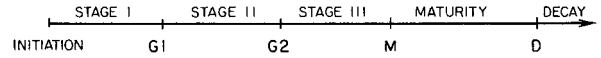


FIG. 4. Time line for MCS evolution as defined in this study. Growth stages: I, II, III, maturity, and decay are labeled along with the stage boundaries (initiation, G1, G2, M, D). Stages I, II, and III have equal durations, averaging ≈2.7 h for this study. See text for definitions.

We define the convective line to include both continuous and discontinuous echoes at the leading edge of the squall line that have cores with peak reflectivities ≥46 dBZ [≈26 mm $h^{-1}$ (Doviak and Zrnić 1993)]. We chose not to use 41 dBZ as the convective threshold since it was considered desirable to have at least one reflectivity range between the convective and stratiform thresholds. This convective threshold is different from the convective threshold of 40 dBZ used in past work (Houze 1977; Zipser 1977; Leary and Houze 1979; Smull and Houze 1985; Leary and Rappaport 1987; Chen and Cotton 1988; Loehrer and Johnson 1995). However, its use in this study is to locate the general orientation of the convective region, not to measure its dimensions. A possible concern of setting the convective threshold to 46 dBZ is that it might discount a substantial portion of the convective line. This does not happen since the 30–40-dBZ elements along the convective line [as determined using animation and comparing to the Houze et al. (1990) conceptual model of an ll–ts MCS] rarely existed without a core with reflectivity ≥46 dBZ. Using a lower threshold might increase the length of the line but it would not significantly alter the orientation or midpoint of the line (characteristics used to assess symmetry and asymmetry).

Thus, although the reflectivity thresholds for distinguishing between stratiform and convective precipitation used in this study are not identical to those used in past studies, they are sufficient for describing the general locations of the two precipitation features and determining the symmetry or asymmetry in the evolving precipitation field.

### *c. Definitions of growth stages*

Our analysis focuses on the early stages of MCS evolution, based in part on the evidence that MCSs tend to evolve to asymmetric systems as they mature (Skamarock et al. 1994; Loehrer and Johnson 1995). Figure 4 depicts the MCS evolution as we refer to it in this study. The evolution of each MCS is partitioned into five periods: growth stage I, growth stage II, growth stage III, maturity, and decay (the average duration of the first four periods, each being about 2.7 h). System characteristics were documented at times separating the five periods: initiation, G1, G2, M, and D. Each period preceding maturity has a duration equal to one-third of the time between initiation and maturity. The evolution was divided this way so that the MCSs could be compared at similar fractions of time into their development.

Determining the time of initiation proved to be the most troublesome of all the stages. The MCSs in this study did not generally evolve steadily from initial convective elements. Rather, the systems generally emerged from a group of convective elements that, at least initially, intensified and decayed without acting as a single system. We decided to approximate the time of initiation under the assumption that a cluster of convection became organized once the cumulative area occupied by the convective precipitation elements began to increase without significant decay, and the spacing between the elements decreased steadily. After examining animations of WSR-88D imagery for the MCSs in this study, the results indicated that once the total area of convective elements (reflectivity >46 dBZ) covered about 8000 $km^2$, the system continued to develop to maturity without significant decaying periods. We therefore define initiation as that time when the total coverage of MCS elements with reflectivity values ≥46 dBZ first covers roughly 8000 $km^2$.

We define maturity as the period during which visual inspection of the reflectivity field revealed that the size and shape of the MCS were nearly constant. Maturity ends when the intensity of the convective line begins to die off, marking the beginning of decay. Table 1 gives the times of initiation and maturity for the 13 cases and the time interval between the two periods.

## 4. Procedures to determine storm symmetry

This analysis of the precipitation field of the MCSs is intended to reveal the gross features, not the details, of the stratiform and convective regions. The features we focus on are those that determine the symmetry of the MCS as described by Houze et al. (1990) (Fig. 1). By their definitions, symmetric systems have a stratiform region centered behind the convective line, and the most intense convective cells have no preferential location along the convective line (R. A. Houze Jr. and B. F. Smull 1996, personal communication). In the Northern Hemisphere, asymmetric systems have a stratiform region located toward the northern end and behind the convective line, and the most intense convective cells preferentially occur toward the southern end of the convective line. The following discussion describes how we applied the symmetric and asymmetric definitions from Houze et al. (1990) to the systems in this analysis.

### *a. Convective line*

The first step in analyzing the convective line was to identify the convective elements of the MCS. Using the WSR-88D composite imagery, we approximated the orientation of the leading convective line with a straight line formed by subjective linear regression of the cells with reflectivities ≥46 dBZ extending the line between the northern most and southern most cells. Figure 5 shows an example of this procedure where all reflectivities are shown in Fig. 5a, but only those exceeding

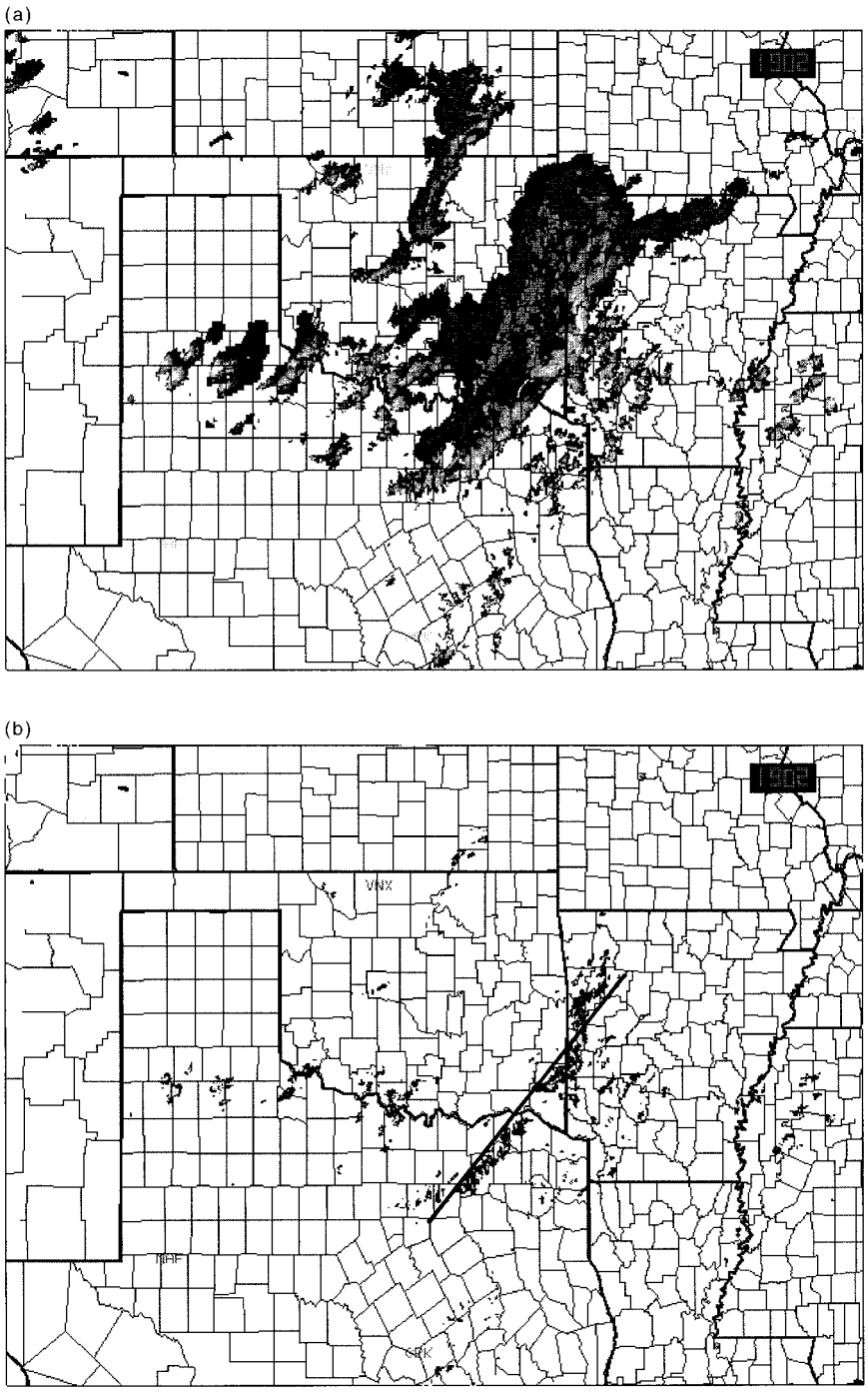


FIG. 5. (a) WSR-88D composite image for 1900 UTC 10 June 1995. (b) WSR-88D reflectivity excluding all returns except those ≥46 dBZ for same time. Convective-line schema (solid line) is formed by fitting the best fit line to the elements with reflectivity ≥46 dBZ. Shading indicates locations with reflectivity >30 dBZ. Shading denotes, from outermost to innermost, 18–29, 30–40, 41–45, 46–49, 50–56, and ≥57 dBZ.

46 dBZ in Fig. 5b. Figure 5b also shows the location of the best-fit convective line resulting from a subjective regression. After documenting the position of the convective line, we focused on the characteristics of the line that determined the nature of the line's symmetry, namely the location and modulation of the most intense convective cells along the length of the convective line. We used 57 dBZ as the threshold for the most intense

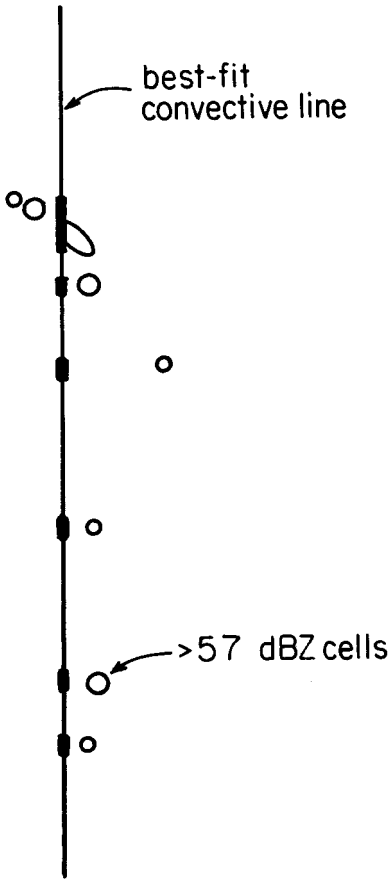


FIG. 6. Schema indicating the location of the most intense convection (≥57 dBZ) along the convective line for 1900 UTC 10 June 1995. Solid lines encompass areas with reflectivity ≥57 dBZ. Thickened segments along convective line are projected locations of most intense convection.

convective elements since that value was the highest-reflectivity threshold offered by the the WSR-88D composites (Table 2).

To document the along-line positions of the most intense convective elements at G1, G2, M, and D, we first outlined the positions of reflectivity regions >57 dBZ at each of those times and then projected these maxima onto the best-fit convective line (Fig. 6). After documenting the locations of the most intense convective cells, we divided each convective line into three major segments of equal length: a northern, a central, and a southern section. We then calculated the fractional coverage of each section by the most intense cells. For example, if 57-dBZ reflectivity covered one-third of the length of the northern section at a particular time, we assigned a value of 33% to the northern section at that time. The average values for each section were then plotted on a histogram to evaluate the composite characteristics of the evolving convective lines.

*b. Stratiform region*

To analyze the stratiform precipitation at G1, G2, and M, we normalized the size of each MCS around a common convective line length. All MCSs were enlarged or reduced in size so that all MCSs had a convective line of the same length (average line length ≈ 400 km). Each normalized reflectivity field valid at G1, G2, and M was placed on a grid (Fig. 7a). A tick mark was placed in each grid square that coincided with a location of a stratiform element (Fig. 7b). After entering all the tick marks for a given system, another system was likewise added to the same grid keeping the location of the convective line the same as the previous system.

The resulting composite indicates the frequency of stratiform precipitation for a given location relative to the convective line at a particular stage of development (Fig. 7c). We then subjectively analyzed frequency of stratiform reflectivity and contoured the analysis to indicate the relative positions of stratiform reflectivity (Fig. 7d).

## 5. Pre-MCS synoptic-scale environments

The axes of the 200-mb jet streaks shown in Fig. 8 indicate that the MCSs generally developed to the east of an upper-level trough within predominantly southwesterly flow aloft, agreeing with past studies (Maddox 1983; Augustine and Howard 1991). This result supports the work of Augustine and Howard (1988) who found that MCSs most frequently occurred east of upper-level troughs where quasigeostrophic (QG) forcing is usually significant. By QG theory, positive-vorticity advection (PVA) forces synoptic lifting, which tends to destabilize the troposphere and may aid in the initiation and maintenance of MCSs. The 500-mb vorticity field analyzed by the National Centers for Environmental Prediction (NCEP; not shown) proved to be inconclusive regarding a preference for either positive or negative vorticity advection accompanying MCS development. This result is due, in part, to the differences in the time of analysis and the time of MCS Initiation, which was often several hours. However, the result is consistent with the findings of Maddox and Doswell (1982), who showed that low-level warm advection is a better indicator of organized, intense convective outbreaks than midtropospheric PVA. The close association between MCS development and low-level warm advection in this study is suggested by later analyses (section 7a) of the frequent occurrence of southerly low-level jets in the MCS analysis region. The locations of the MCSs coincide with areas that are close to the 200-mb jet entrance or exit (Fig. 8). The MCS–initiation environments comprise a diversity of 200-mb jet patterns (i.e., both exit and entrance regions) and three MCSs (4, 27, and 29 June) occurred on days without a significant upper-level jet near the analysis region. Note that only one location for the 200-mb jet is used in Fig.

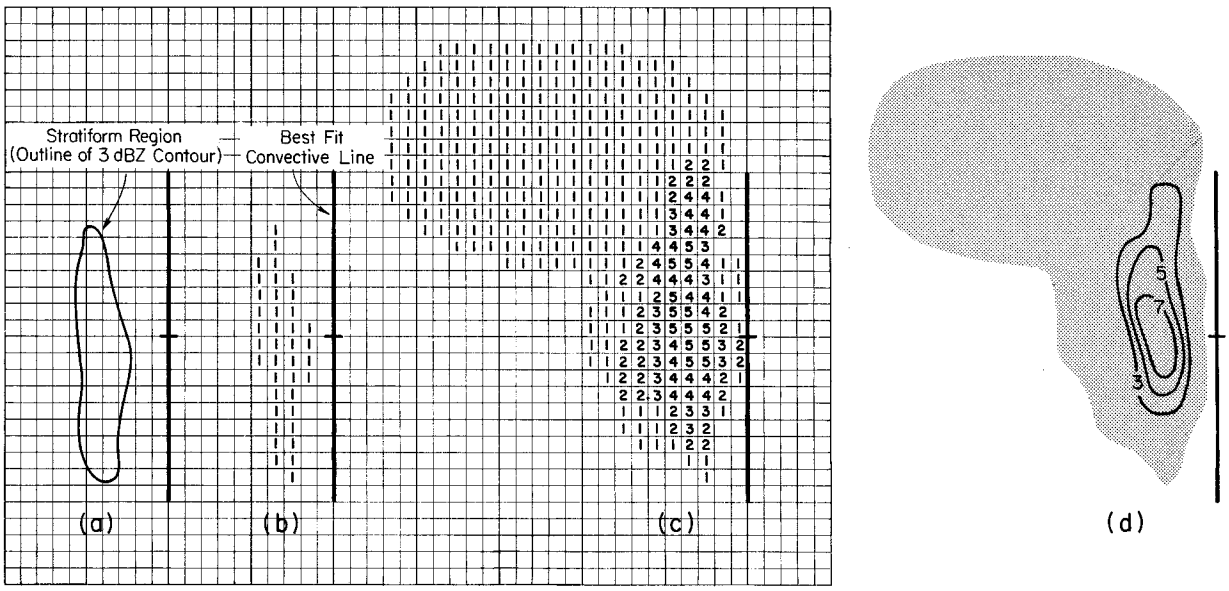


FIG. 7. An example of creating a stratiform composite. (a) First step: outlining stratiform region with best-fit, normalized convective line drawn on grid. (b) Second step: placing of tick marks to represent the location of stratiform elements relative to the normalized convective line. (c) Third step: tallying the frequency of tick marks after accounting for all MCSs. (d) Subjectively analyzed field corresponding to (c). Shaded region represents a frequency of at least one; contours represent the percent of MCSs having stratiform reflectivity (>30 dBZ) at a location relative to the convective line. Contours are 30%, 50%, and 70%. Composite grid spacing is approximately 20 km × 20 km.

8 for each of the two days with more than one MCS (3 June, 10 June). These findings imply that the formation of MCSs is not intimately tied to jet dynamics aloft (e.g., Maddox 1983). There is, however, an association between MCS development and the LLJ. Since the LLJ is also related to the evolution of MCSs into asymmetric systems, the LLJ is discussed later (section 7a).

In agreement with past studies (Merritt 1985; Fritsch et al. 1986; Maddox 1980, 1983; Bluestein and Jain 1985; Bluestein et al. 1987; Augustine and Howard 1991; Loehrer and Johnson 1995), the MCSs in this study frequently appeared in association with surface frontal zones. Of the 13 MCSs, 6 formed when a cold or stationary front was stretched across the analysis region (as indicated by NCEP analysis[3]) within 250 km of the MCS (Fig. 9).

## 6. Observations of the reflectivity field

We began our observations with the intention of documenting precipitation patterns during each MCS's evolution using criteria for patterns set forth by Houze et al. (1990). Their definitions of symmetric and asymmetric systems rest upon two basic characteristics of the precipitation structure: 1) the location of the most intense convective cells along the convective line, and 2) the position of the stratiform region relative to the center of the convective line. Our analysis revealed that the systems frequently exhibited a mixture of indicators for symmetry/asymmetry. For example, 60% of the observations were convective lines with asymmetric characteristics and stratiform regions with symmetric characteristics, and vice versa. Therefore, at each stage in its evolution the precipitation pattern of each MCS was usually not classifiable as strictly symmetric or asymmetric.

Since the classification of the entire MCS was often ambiguous, we examined each precipitation component, convective and stratiform, to determine whether they were individually symmetric or asymmetric. As before, these assignments are based on the definitions described by Houze et al. (1990). The convective component is assigned as 1) asymmetric if the most intense convective cells were predominately to one end of the convective line, and 2) symmetric if the most intense cells were clustered toward the midpoint of the convective line or were evenly distributed along the line. The stratiform component is assigned as 1) asymmetric if the centroid of the stratiform region was located toward the northern end of the convective line, and 2) symmetric if the centroid was more or less centered behind the midpoint of the convective line. In order to apply these definitions objectively, we had to determine a threshold that defined which centroid positions were and were not centered behind the convective line. After analyzing the MCSs, it became apparent that slight changes in the threshold significantly changed the distribution of symmetric and asymmetric systems. Thus, using a threshold introduced

[3] Sanders and Doswell (1995), however, found that NCEP-analyzed fronts may at times not reflect the true surface thermal discontinuities.

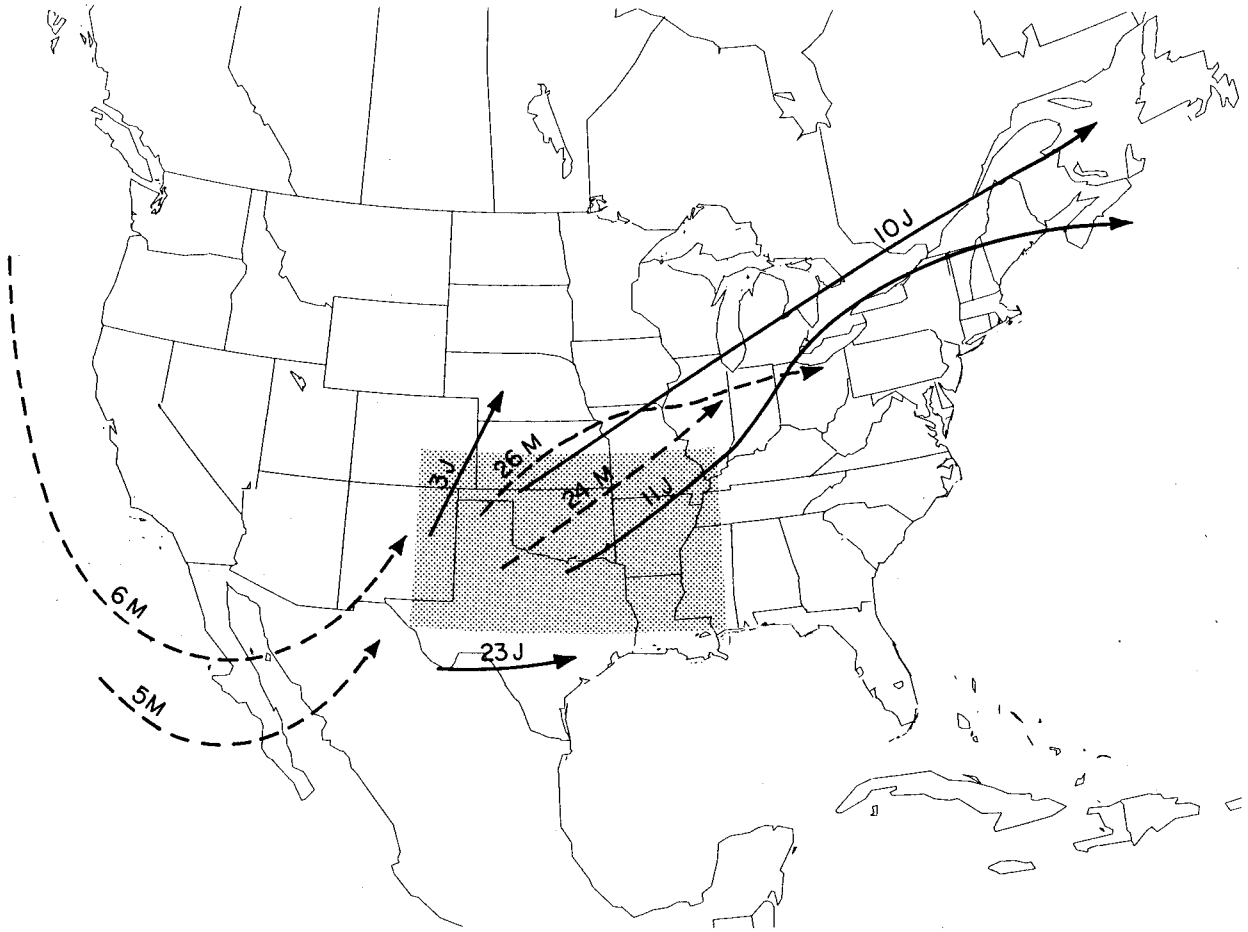


FIG. 8. Jet streaks at 200 mb as analyzed by the NWS valid during each MCSs Maturity stage. Solid lines (dashed lines) represent position of jet core with average speed of 36 m $s^{-1}$ ($\geq$40 m $s^{-1}$). Shaded region is analysis region for this study. Day and month are labeled above each arrow (e.g., 24M is 24 May, 10J is 10 June).

an undesirable level of arbitrariness in the results. Therefore, rather than using strict definitions for symmetry or asymmetry for the precipitation patterns at each stage of each MCS, we merged the reflectivity distributions for all MCSs into a composite and then subjectively assessed whether the composite patterns were generally symmetric or asymmetric.

Figure 10 reveals the average fraction of each section of the convective line (north, center, and south) comprising the most intense cells (>57 dBZ) at specific times (G1, G2, M, D) for the 13 MCS cases. There is a trend for the percentage within the northern section to decrease with time and the percentage for the southern section to increase with time. This tendency toward asymmetry in the convective line is consistent with the modeling study of Skamarock et al. (1994). Also noteworthy, there does not appear to be a preferential location for intense cells at times G1, G2, and M. By decay, however, there is some suggestion that the most intense cells are preferentially located along the southern third of the convective lines, an asymmetric characteristic.

Figure 11 shows the frequency of stratiform precipitation at locations relative to the convective line. Early in the MCS evolution (G1), in a composite sense, MCSs displayed a preference for the stratiform precipitation to occur almost directly behind the midpoint of the convective line, a characteristic of a symmetric system. By G2, a definite shift toward an asymmetric pattern is evident. This pattern of stratiform locations is nearly constant from G2 to M. One of the differences between the composites valid at G2 and M is that stratiform elements extend farther north of the convective line at M than for G2. Also, there is a southward shift of the 50% contour, perhaps reflecting hydrometeor transport (e.g., Biggerstaff and Houze 1991) from strong cells developing on the southern part of the line at time M (Fig. 10).

Thus, in a composite sense, the MCSs indicated a preference for symmetric characteristics early in their evolution and asymmetric characteristics toward the end of their evolution. This is consistent with the observations of Loehrer and Johnson (1995) and confirms to the modeling work of Skamarock et al. (1994). How-

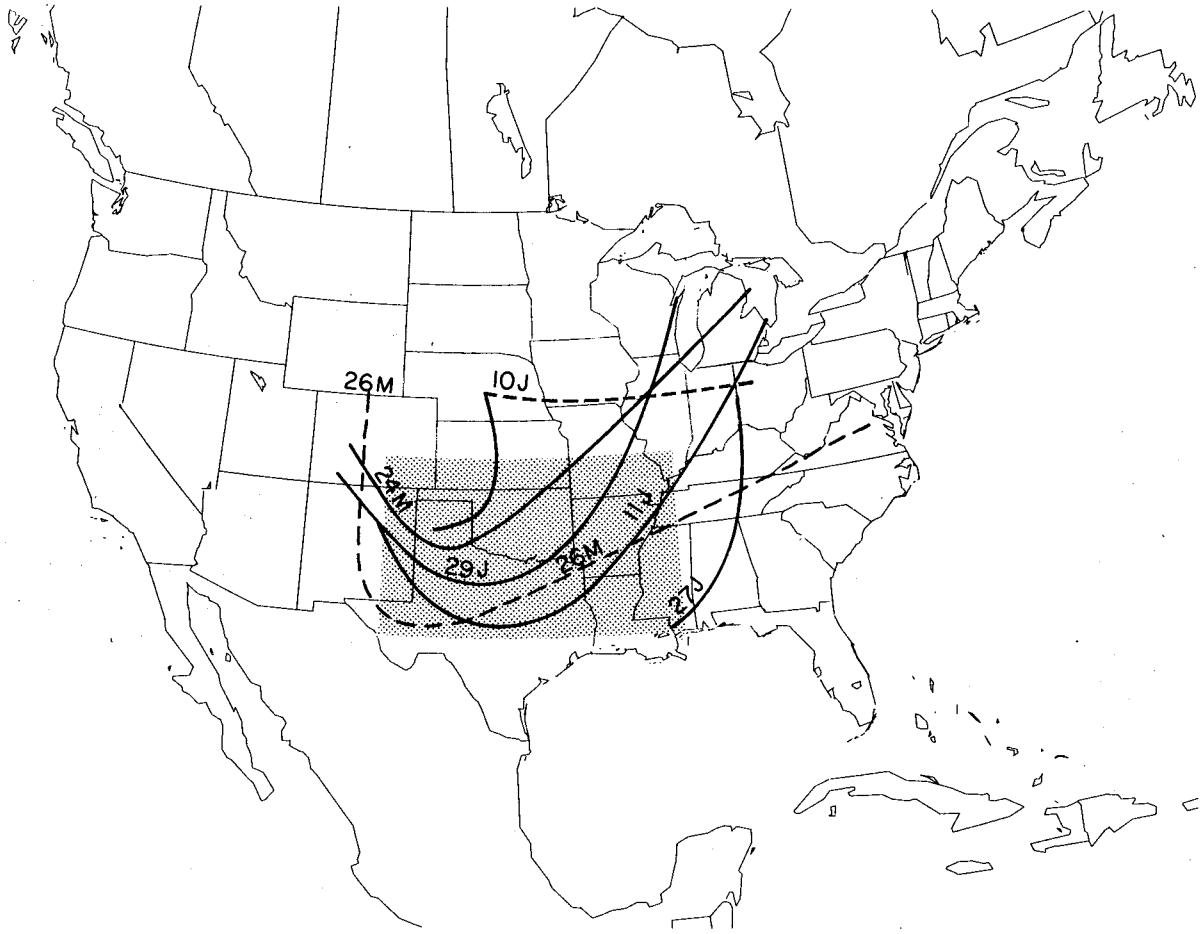


FIG. 9. Locations of cold fronts (solid) and stationary fronts (dashed) valid during each MCSs maturity. Fronts are located at the position reported on NWS synoptic charts. Shaded region is analysis region for this study. Day and month are labeled above each frontal position (e.g., 24M is 24 May, 10J is 10 June).

ever, the results (admittedly from a limited sample) suggest that the stratiform region evolves toward asymmetry at least one full category (≈2.5–3 h) prior to the convective line. The implications of this result are not clear and require further verification with additional observational studies.

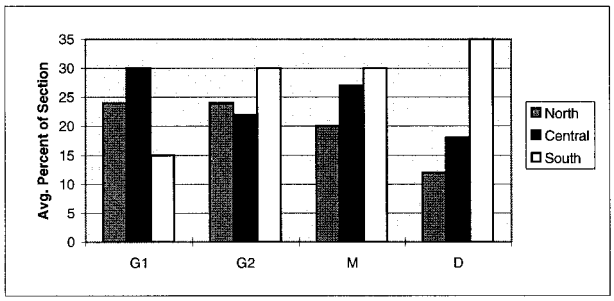


FIG. 10. Frequency of the most intense (≥57 dBZ) cell locations at the northern-, central-, and southern-most thirds of the convective line. Frequencies are given for G1, G2, M, and D. See Fig. 4 for explanation of times.

## 7. Factors contributing to asymmetry

Houze et al. (1990) attributed squall-line asymmetry to along-line vertical wind sheer, which produces differing flow environments for cells along the southern and northern ends of the convective line. In the modeling study of Skamarock et al. (1994), the tendency for MCSs to evolve toward asymmetry as they matured was attributed to two primary factors: 1) the Coriolis force acting on the ascending front-to-rear flow in the convective line, turning it to the north and leading to an accumulation of hydrometeors and positively buoyant air there, and 2) the Coriolis force acting on rear-to-front flow within the surface cold pool, driving cold air to the south and generating new cells preferentially on the southern end of the line. Smull and Augustine (1993) explained the creation of asymmetric MCSs arguing that the LLJ provides southerly momentum to updrafts where it is transported aloft and advects hydrometeors northward from the convective towers. Both these theories require system-relative along-line flows to form an asymmetric MCS. In an attempt to simulate the evo-

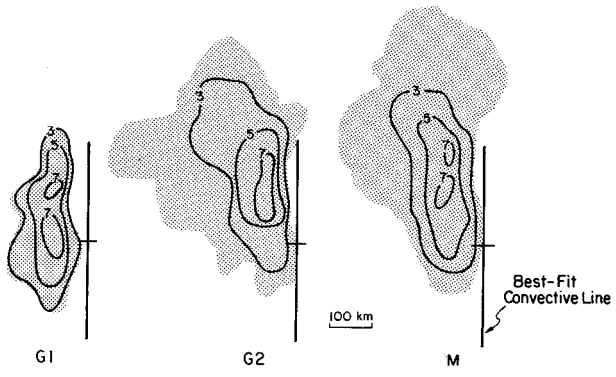


FIG. 11. Stratiform reflectivity composites for G1, G2, and maturity (average time separation = 2.7 h). Convective line with midpoint position are given. Contours represent percent of MCSs having stratiform reflectivity (>30 dBZ) at a location relative to the convective line. Contours are 30%, 50%, and 70%. Shaded region indicates those locations that had at least one occurrence of stratiform reflectivity. The 100-km scale is based on the average MCS size.

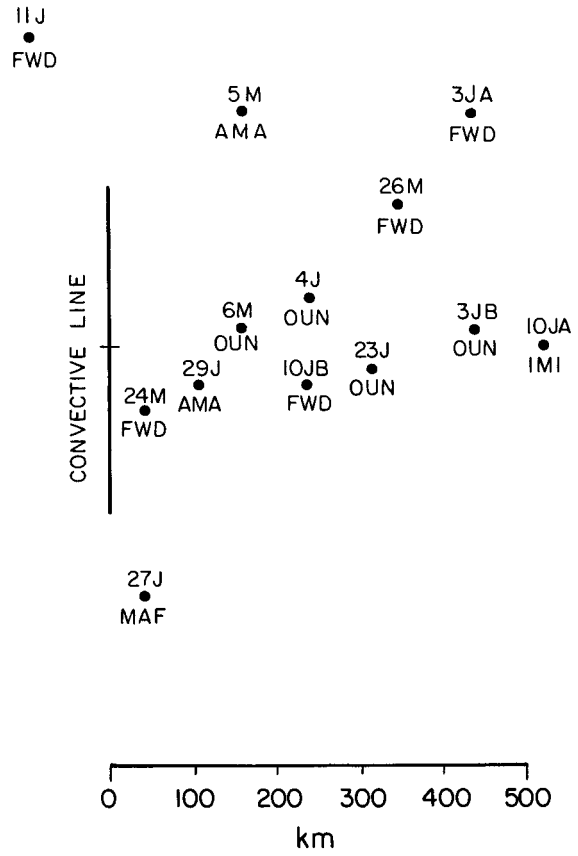


FIG. 12. Locations of soundings relative to the convective line used to create along- and cross-line wind profiles. Convective line schema and distance scale are given. Date and NWS station listed for each sounding location. Date is day of month followed by the first letter of the month (M-May, J-June). Station identification is that used by the NWS. See Fig. 3 for locations of upper-air stations.

lution of the MCS precipitation structure, Skamarock et al. (1994) simplified the environmental flow to one dimension, namely, perpendicular to the initial north–south convective line. It is well known, however, that most squall lines occur in environments characterized by both line-perpendicular and line-parallel ambient flow (Houze et al. 1990). The role of the line-parallel component of the flow in MCS asymmetry is explored next.

### *a. Storm-relative environmental flow*

Environmental, storm-relative flow was determined by using one sounding for each MCS to represent its pre-MCS environment. The locations of all such soundings relative to the convective line are shown in Fig. 12 and the times of each sounding are given in Table 1. Sounding positions range from within 100 km of the convective line to over 500 km from the convective line. The soundings used were those closest to the environment through which the MCS passed during its evolution. While 0000 and 1200 UTC soundings are the only ones available, their winds are regarded as representative of the ambient winds during the passage of the MCSs since the presquall, upper-level winds are not expected to change significantly over the life of the average MCS in this study (≈8 h). Of course, it is well known that the upper- and lower-level flow can change dramatically within MCSs over their life cycles (Fritsch and Maddox 1981).

The along-line wind profiles for each case and their mean are illustrated in Fig. 13. Positive (negative) values represent motion from the south (north). Although there is considerable scatter, the average profile is positive through the entire troposphere, increasing from the boundary layer to a maximum of about 10 m $s^{-1}$ near 150 mb and then decreasing aloft. This profile is consistent with the common location of the MCSs in this study, east of a trough in predominantly southwesterly flow (Fig. 8). Since the MCSs in this study often had convective lines oriented roughly north–south, southwesterly flow aloft produces a positive, system-relative, along-line flow. This flow increases with height, consistent with the existence of a baroclinic zone associated with a trough to the west. Negative, system-relative flows in the lowest 150 mb may arise from the usual (9 of 13 MCSs) southwest-to-northeast orientation of the convective lines and the easterly component of the system-relative, presquall low-level flow. This easterly component can be explained by the location of some MCSs to the north of fronts.

The cross-line wind profiles for each case and their mean are illustrated in Fig. 14. Positive (negative) values represent rear-to-front (RTF) [front-to-rear (FTR)] flows. The average profile is predominately negative indicating that the lower and midtroposphere are dominated by FTR flows (e.g., Zipser 1977; Augustine and Howard 1991). The strongest FTR flow occurs near the surface with the profile becoming less negative with

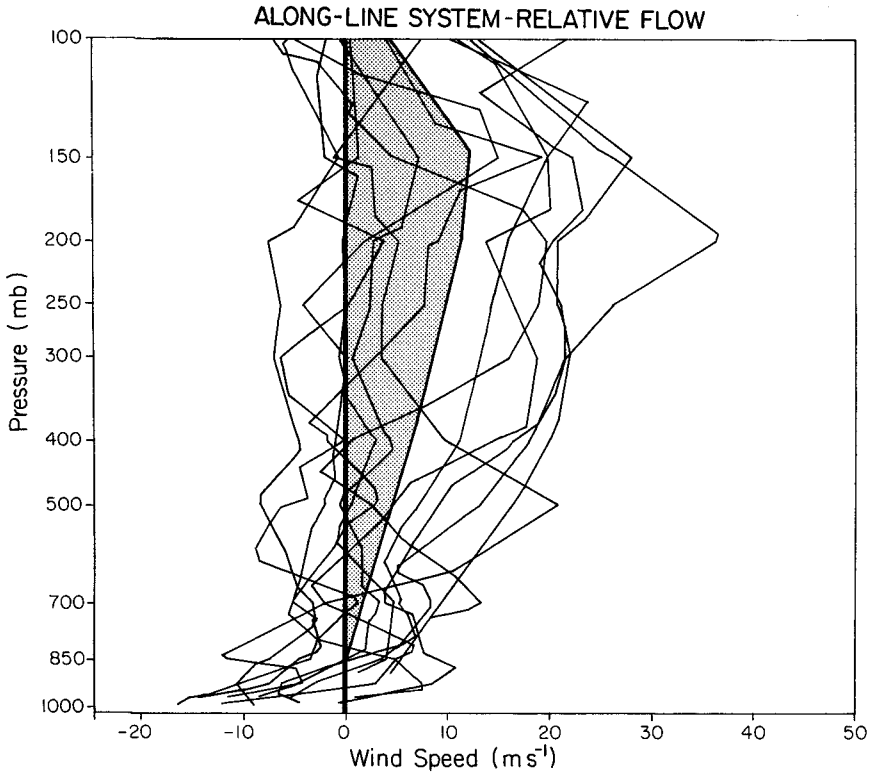


FIG. 13. Wind profile for along-line, system-relative flows. Positive speed is toward the north. Thick line is the average profile. Shading is from zero line to profile-average line.

height and exhibiting a shallow layer of RTF flow near 175 mb. The average RTF flow just above 200 mb may reflect an upper-level west-to-southwesterly jet, or in a few instances (6 May, 24 May, 29 June) the MCS outflow in the leading anvil as depicted in the conceptual model presented in Houze et al. (1989, their Fig. 1). The surface-to-tropopause cross-line shear is nearly the same as the along-line shear ($\approx 1.5 \times 10^{-3}$ s$^{-1}$). Combining the along-line and cross-line components of vertical shear gives an average total shear of $2.1 \times 10^{-3}$ s$^{-1}$, which is comparable to the surface-to-tropopause shears observed in Bluestein and Jain (1985) for severe squall lines ($3.1 \times 10^{-3}$ s$^{-1}$), and Bluestein et al. (1987) for nonsevere squall lines ($2.8 \times 10^{-3}$ s$^{-1}$), and the 0–6 km shears of 2.5 and $2.9 \times 10^{-3}$ s$^{-1}$ for symmetric and asymmetric MCSs observed by Houze et al. (1990).

The LLJ appears to be active at the time of each MCS initiation. Figure 15 is an analysis of the 850-mb LLJ axis, subjectively analyzed from the NWS upper-air soundings closest in time and location to the formation of the MCSs. This analysis indicates a recurrence of a southerly LLJ, consistent with the observations in previous studies and suggesting that low-level warm advection was an important contributor to the forcing of vertical motion in a number of the cases (Maddox and Doswell 1982; Maddox 1983).

### *b. Implications of system-relative flows*

A number of studies (e.g., Hobbs et al. 1980; Matejka and Hobbs 1981; Smull and Houze 1985; Biggerstaff and Houze 1991; Smull and Augustine 1993) have explained the existence of the secondary band of precipitation (or trailing stratiform region) as a consequence of the rearward advection of snow and ice in the FTR flow aloft from the leading convective line. Using fall speed estimates for the types of hydrometeors encountered and considering observed vertical velocities in the stratiform region, they find that hydrometeor trajectories extend 100–200 km behind the line. However, the results shown in Figs. 13 and 14 show that at 500 mb the storm-relative along-line flow is just as strong as the FTR flow. Above 500 mb the along-line flow is even stronger than the cross-line flow. Moreover, the environmental low-level flow (Fig. 15) comprising the LLJ is likely providing strong southerly momentum to the storm inflow (e.g., Smull and Augustine 1993), which translates into south-southeasterly storm-relative flow for eastward moving MCSs. Therefore, one can expect hydrometeor transport in the along-line direction (toward the north) to be at least as great or even greater than transport to the rear. This two-dimensional storm-relative flow will obviously contribute to an asymmetric

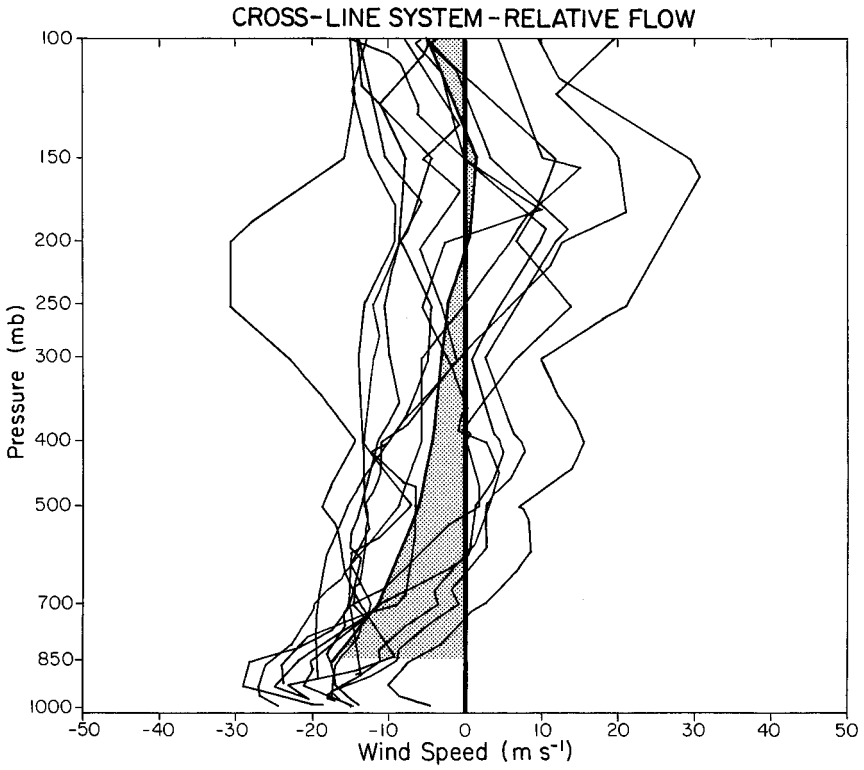


FIG. 14. Same as Fig. 13 except for cross-line, system-relative flows. Positive speed is rear to front.

distribution of stratiform precipitation skewed toward the northern end of the system.

Although the pre-MCS environment may have shear that promotes advection northwest of the line center, the ambient shear is probably considerably modified by the MCS (e.g., Fritsch and Maddox 1981). Thus, the shear that advects the hydrometeors is likely a combination of ambient conditions and the effects of the MCSs themselves (Skamarock et al. 1994).

## 8. Summary and conclusions

Thirteen MCSs that occurred during May and June 1995 within Texas and Oklahoma were examined in this study using WSR-88D animations. The MCS environments were similar to those found in past studies: regions likely influenced by strong quasi-geostrophic and frontal forcing.

The reflectivity fields were examined to assess how the precipitation patterns of the MCSs evolved. This study is intended as an extension of past studies of MCS symmetry (e.g., Houze et al. 1990; Loehrer and Johnson 1995) and to address the theory that the precipitation structure of an MCS is due in part to the advection of hydrometeors (Hobbs et al. 1980; Matejka and Hobbs 1981; Smull and Houze 1985; Biggerstaff and Houze 1991) in addition to Coriolis effects (Skamarock et al. 1994). The analysis focused on the traits of symmetric and asymmetric MCSs as defined by Houze et al. (1990). The majority of the MCSs in this study did not exhibit a precipitation pattern that was entirely symmetric or asymmetric. Therefore, rather than attempting to assign each system as symmetric or asymmetric at each stage during its evolution, we isolated the convective and stratiform regions of each MCS and analyzed composites of each region over all 13 MCSs. We defined the convective line to include both continuous and discontinuous echoes at the leading edge of the squall line that had cores with peak reflectivities $\geq$46 dBZ. We defined the stratiform region to be that part of the precipitation field separate from the convective line and having a nearly contiguous region of reflectivity $\geq$30 dBZ. We used 57 dBZ as the reflectivity threshold for identifying the most-intense convective cells and hence examined their tendency to be preferentially located along a given portion of the convective line.

In a composite sense, both the convective line and stratiform region evolved from symmetric structures to asymmetric structures. Upon reaching maturity the stratiform region exhibited a preference to be located to the northern end of the system. At this time, the convective line also exhibited asymmetric characteristics, having a concentration of the most intense convective cells along the southern end of the convective line. These results are consistent with the observations of Loehrer and Johnson (1995) and the modeling work of Skamarock

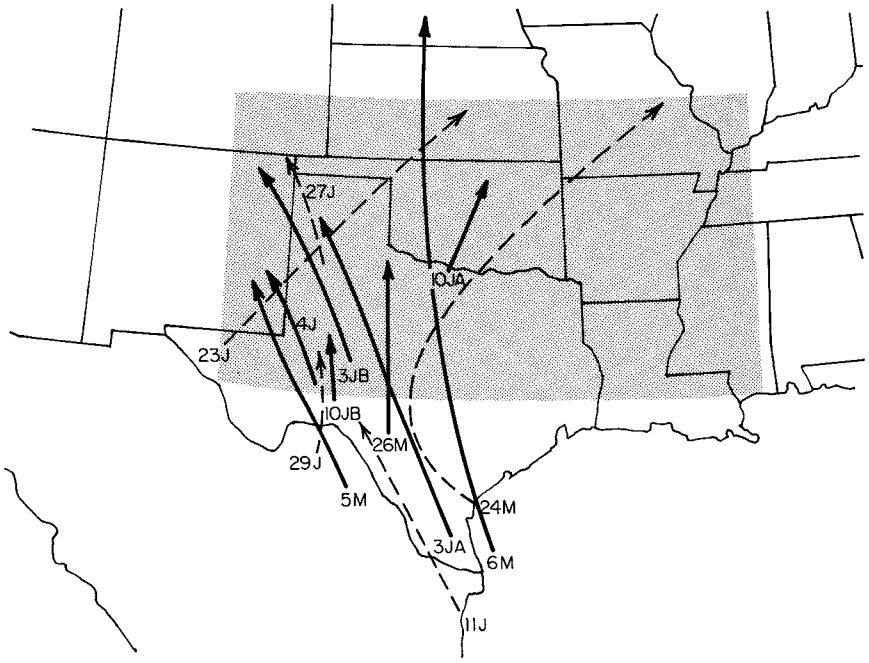


FIG. 15. The 850-mb low-level jet locations subjectively analyzed using the NWS soundings. Solid (dashed) lines represent locations of a jet with a maximum speed $\geq$15 m s$^{-1}$ ($\geq$10 m s$^{-1}$). Day and month are labeled along side or at the origin of each arrow. Shaded region is analysis region for this study.

et al. (1994). In addition to the information provided in these past works, our results indicate that the transition from symmetric to asymmetric characteristics for the stratiform region occurs on average 2–3 h before the convective line exhibits asymmetric characteristics, although these results are for a very small sample.

Modeling studies of MCSs that attempted to determine the reason for the transition from symmetric to asymmetric systems (e.g., Skamarock et al. 1994) initialized their models without along-line flow (i.e., using only cross-line shear). Similarly, other studies have focused on the cross-line flows within the pre-MCS environment in an attempt to explain the existence of the stratiform region (e.g., Matejka and Hobbs 1981; Smull and Houze 1985; Biggerstaff and Houze 1991; Smull and Augustine 1993). As an extension of these works, our results indicate that the system-relative, along-line flows (toward the north) are as strong or stronger than the cross-line flows within the pre-MCS environment, consistent with the findings of Houze et al. (1990). This result supports the idea that both along-line and cross-line flows contribute to an asymmetric distribution of stratiform precipitation skewed toward the northern end of an MCS. This is not to say, however, that the ambient conditions dictate the final precipitation structure of MCSs. Rather, the precipitation structure is likely due to a combination of ambient flows, and the effects of MCSs that respond to Coriolis and other forcing effects.

Since these results are from a limited sample, continued investigation of MCS evolution is necessary for confirmation. Future research is required to increase the sample size, and modeling studies are needed to determine the sensitivity of the final precipitation structure to the two-dimensional shear of the pre-MCS environment.

*Acknowledgments.* The authors wish to thank Professor Kenneth Crawford, director of the Oklahoma Climatological Survey, and Mark Schafer and Dale Morris at the University of Oklahoma at Norman for their help in acquiring the data used in this study. Also appreciated are the helpful comments provided by Professor Steven A. Rutledge and two anonymous reviewers. This research was supported by the National Science Foundation under Grant ATM-9313716 and a fellowship awarded by the American Meteorological Society and ITT Aerospace Communications Division.

## REFERENCES

Augustine, J. A., and K. W. Howard, 1988: Mesoscale convective complexes over the United States during 1985. *Mon. Wea. Rev.,* **116,** 685–701.

——, and ——, 1991: Mesoscale convective complexes over the United States during 1986 and 1987. *Mon. Wea. Rev.,* **119,** 1575–1589.

Biggerstaff, M. I., and R. A. Houze Jr., 1991: Kinematic and precipitation structure of the 10–11 June 1985 squall line. *Mon. Wea. Rev.,* **119,** 3034–3065.

Bluestein, H. B., and M. H. Jain, 1985: Formation of mesoscale lines of precipitation: Severe squall lines in Oklahoma during spring. *J. Atmos. Sci.,* **42,** 1711–1732.

——, G. T. Marx, and M. H. Jain, 1987: Formation of mesoscale lines of precipitation: Nonsevere squall lines in Oklahoma during the spring. *Mon. Wea. Rev.,* **115,** 2719–2727.

Brandes, E. A., 1990: Evolution and structure of the 6–7 May 1985 mesoscale convective system and associated vortex. *Mon. Wea. Rev.,* **118,** 109–197.

Chen, S., and W. R. Cotton, 1988: The sensitivity of a simulated extratropical mesoscale convective system to longwave radiation and ice-phase microphysics. *J. Atmos. Sci.,* **45,** 3897–3910.

Collier, C. G., S. Lovejoy, and G. L. Austin, 1980: Analysis of bright bands from 3D radar data. Preprints, *19th Conf. on Radar Meteorology,* Miami Beach, FL, Amer. Meteor. Soc., 44–47.

Cunning, J. B., 1986: The Oklahoma–Kansas preliminary regional experiment for STORM-Central. *Bull. Amer. Meteor. Soc.,* **67,** 1478–1486.

Davis, C. A., and M. L. Weisman, 1994: Balanced dynamics of mesoscale vortices produced in simulated convective systems. *J. Atmos. Sci.,* **51,** 2005–2030.

Doswell, C. A., III, H. E. Brooks, and R. A. Maddox, 1996: Flash flood forecasting: An ingredients-based methodology. *Wea. Forecasting,* **11,** 560–581.

Doviak, R. J., and D. S. Zrnić, 1993: *Doppler Radar and Weather Observations.* 2d ed. Academic Press, 562 pp.

Fritsch, J. M., and R. A. Maddox, 1981: Convectively driven mesoscale weather systems aloft. Part 1: Observations. *J. Appl. Meteor.,* **20,** 9–19.

——, R. J. Kane, and C. R. Chelius, 1986: The contribution of mesoscale convective weather systems to the warm-season precipitation in the United States. *J. Climate Appl. Meteor.,* **25,** 1333–1345.

Fujita, T., 1955: Results of detailed synoptic studies of squall lines. *Tellus,* **7,** 405–436.

Hobbs, P. V., T. J. Matejka, P. H. Herzegh, J. D. Locatelli, and R. A. Houze Jr., 1980: The mesoscale and microscale structure and organization of clouds and precipitation in midlatitude cyclones. I: A case study of a cold front. *J. Atmos. Sci.,* **37,** 568–596.

Houze, R. A., Jr., 1977: Structure and dynamics of a tropical squall-line system. *Mon. Wea. Rev.,* **105,** 1540–1567.

——, 1993: *Cloud Dynamics.* Academic Press, 573 pp.

——, S. A. Rutledge, M. I. Biggerstaff, and B. F. Smull, 1989: Interpretation of Doppler weather radar displays of midlatitude mesoscale convective systems. *Bull. Amer. Meteor. Soc.,* **70,** 608–619.

——, B. F. Smull, and P. Dodge, 1990: Mesoscale organization of springtime rainstorms in Oklahoma. *Mon. Wea. Rev.,* **118,** 613–654.

Johns, R. H., and W. D. Hirt, 1987: Derechos: Widespread convectively induced windstorms. *Wea. Forecasting,* **2,** 32–49.

Knupp, K. R., and W. R. Cotton, 1987: Internal structure of a small mesoscale convective system. *Mon. Wea. Rev.,* **115,** 629–645.

Leary, C. A., and R. A. Houze Jr., 1979: The structure and evolution of convection in a tropical cloud cluster. *J. Atmos. Sci.,* **36,** 437–457.

——, and E. N. Rappaport, 1987: The life cycle and internal structure of a mesoscale convective complex. *Mon. Wea. Rev.,* **115,** 1503–1527.

Ligda, M. G. H., 1951: Radar storm observation. *Compendium of Meteorology,* T. F. Malone, Ed., Amer. Meteor. Soc., 1265–1282.

Loehrer, S. M., and R. H. Johnson, 1995: Surface pressure and precipitation life cycle characteristics of PRE-STORM mesoscale convective systems. *Mon. Wea. Rev.,* **123,** 600–621.

Maddox, R. A., 1980: Mesoscale convective complexes. *Bull. Amer. Meteor. Soc.,* **61,** 1374–1387.

——, 1983: Large-scale meteorological conditions associated with midlatitude mesoscale convective complexes. *Mon. Wea. Rev.,* **111,** 1475–1493.

——, and C. A. Doswell III, 1982: An examination of jet stream configurations, 500-mb vorticity advection and low-level thermal advection patterns during extended periods of intense convection. *Mon. Wea. Rev.,* **110,** 184–197.

Matejka, T. J., and P. V. Hobbs, 1981: The use of a single Doppler radar in short-range forecasting and real-time analysis of extratropical cyclones. *Proc. IAMAP Symp. on Nowcasting: Mesoscale Observation and Short-Range Prediction,* Hamburg, Germany, Int. Association of Meteorology and Atmospheric Physics, 177–181.

Merritt, J. H., 1985: The synoptic environment and movement of mesoscale convective complexes over the United States. M.S. thesis, Dept. of Meteorology, The Pennsylvania State University, 129 pp.

Newton, C. W., 1950: Structure and mechanism of the pre-frontal squall line. *J. Meteor.,* **7,** 210–222.

——, and H. R. Newton, 1959: Dynamical interactions between large convective clouds and environments with vertical shear. *J. Meteor.,* **16,** 483–496.

Pedgley, D. E., 1962: *A Meso-Synoptic Analysis of the Thunderstorms of 28 August 1958.* Geophysical Memoirs, Vol. 14, Brit. Meteor. Office, 74 pp.

Rutledge, S. A., R. A. Houze Jr., M. I. Biggerstaff, and T. Matejka, 1988: The Oklahoma–Kansas mesoscale convective system of 10–11 June 1985: Precipitation structure and single-Doppler radar analysis. *Mon. Wea. Rev.,* **116,** 1409–1430.

Sanders, F., and R. J. Paine, 1975: Structure and thermodynamics of an intense mesoscale convective storm in Oklahoma. *J. Atmos. Sci.,* **32,** 1563–1579.

——, and K. A. Emanuel, 1977: The momentum budget and temporal evolution of a mesoscale convective system. *J. Atmos. Sci.,* **34,** 322–330.

——, and C. A. Doswell III, 1995: A case for detailed surface analysis. *Bull. Amer. Meteor. Soc.,* **76,** 505–521.

Scott, J. D., and S. A. Rutledge, 1995: Doppler radar observations of an asymmetric mesoscale convective system and associated vortex couplet. *Mon. Wea. Rev.,* **123,** 3437–3457.

Skamarock, W. C., M. L. Weisman, and J. B. Klemp, 1994: Three-dimensional evolution of simulated long-lived squall lines. *J. Atmos. Sci.,* **51,** 2563–2584.

Smull, B. F., and R. A. Houze Jr., 1985: A midlatitude squall line with a trailing region of stratiform rain: Radar and satellite observations. *Mon. Wea. Rev.,* **113,** 117–133.

——, and J. A. Augustine, 1993: Multiscale analysis of a mature mesoscale convective complex. *Mon. Wea. Rev.,* **121,** 103–132.

Steiner, M., R. A. Houze, and S. E. Yuter, 1995: Climatological characterization of three-dimensional storm structure from operational radar and rain gauge data. *J. Appl. Meteor.,* **34,** 1978–2007.

Trier, S. B., and D. B. Parsons, 1993: Evolution of environmental conditions preceding the development of a nocturnal mesoscale convective complex. *Mon. Wea. Rev.,* **121,** 1078–1098.

Zipser, E. J., 1977: Mesoscale and convective-scale downdrafts as distinct components of squall-line circulation. *Mon. Wea. Rev.,* **105,** 1568–1589.

——, 1982: Use of a conceptual model of the life cycle of mesoscale convective systems to improve very-short-range forecasts. *Nowcasting,* K. Browning, Ed., Academic Press, 191–204.